

# High-Power Single-Mode ZnO Thin-Film Random Lasers

S. F. Yu, *Senior Member, IEEE*, and Eunice S. P. Leong

**Abstract**—The possibilities to realize high-power single-mode ultraviolet lasing in highly disordered zinc oxide (ZnO) thin films are investigated. An effective one-dimensional time-domain traveling-wave model is developed to simulate random laser action in ZnO thin-film waveguides with ridge structure. Spectral and spatial redistributions of lasing modes, due to lasing mode localization and repulsion, are shown in highly disordered media. Hence, by controlling the photon density distribution, selective excitation of lasing modes can be achieved. A coupled-cavity ZnO thin-film random laser is also proposed to achieve high-power single-mode operation under nonuniform pumping. Preliminary experimental results have verified the possibility to realize high-power single-mode emission by the use of the proposed coupled-cavity design.

**Index Terms**—Random lasing action, semiconductor laser modeling, zinc oxide (ZnO) thin films.

## I. INTRODUCTION

**R**ANDOM LASER action in ultraviolet (UV) has been observed in different forms of zinc oxide (ZnO), such as powder [1], thin film [2] and cluster [3]. As ZnO powder and cluster are difficult to handle, ZnO thin films may be a better choice to realize practical UV lasers. This is because the highly disordered thin films can: 1) allow the formation of optical waveguide to minimize nonaxial scattering of lasing light; 2) avoid the difficulty in cleaving smooth facets to sustain lasing; and 3) achieve electrical pumping to generate high-intensity random lasing [4]. However, multimode operation, which is an undesirable characteristic of ideal lasing sources, is unavoidable in highly disordered ZnO thin films under high excitation. Injection locking [5] can be used to constrain single-mode oscillation in highly disordered ZnO thin films but this is not a simple technique to obtain practical UV lasers. Selective excitation of individual localized modes [6] has also been proposed to realize single-mode operation in random media. Nevertheless, the requirement of small excitation area and low pump rate will not allow high-power performance. Therefore, it is required to further investigate the random lasing action in highly disordered ZnO thin films in order to deduce a simpler technique to realize high-power single-mode operation.

Finite-difference time-domain (FDTD) method has been applied to solve Maxwell's equation and rate equation of electron population self-consistently for the investigation of random

lasing in highly disordered media [6], [7]. Recent development of one-dimensional (1-D) FDTD model, which has shown high computational efficiency, can reproduce key aspects of experimental observation such as localization, repulsion, and saturation of lasing modes [7]. However, the use of ZnO thin-film random lasers for practical applications requires long cavity design (i.e., also requires long computational time to analyze) because of the ease in handling, high output power and low pump threshold. Therefore, it may be necessary to further improve the computational efficiency of the 1-D FDTD method to facilitate future studies on ZnO random lasers for practical applications.

In this paper, we study the possibilities to achieve high-power single-mode UV emission from highly disordered ZnO thin films. A 1-D time-domain traveling-wave model is developed to investigate the random laser action in ZnO thin films. Spatial and spectral distributions of lasing modes are calculated using time-dependent transfer-matrix method. Improvement in computational efficiency over the conventional 1-D FDTD method can be obtained by using transfer matrix to increase the sampling size but without reducing the stability and calculation accuracy. The proposed model has shown agreement with analogous calculations given in [7] and experimental results demonstrated in [2]. Using the model, the behavior of spectral and spatial redistributions of lasing modes in highly disordered media is explained. It is shown that selective excitation of lasing modes can be obtained by controlling the photon density distribution. A coupled-cavity random laser, which consists of a traveling-wave amplifier (TWA) and a short random cavity, is proposed to achieve high-power single-mode operation. The influence of optical feedback and nonuniform optical pumping on the modal selection mechanism is also analyzed. The coupled-cavity ZnO thin-film random laser has been fabricated by the filtered cathodic vacuum arc (FCVA) technique and the corresponding lasing characteristics are studied experimentally.

## II. THEORETICAL MODEL OF 1-D ZnO RANDOM LASERS

Fig. 1 shows the scan electron microscope (SEM) image of a highly disordered ZnO thin film. The nonuniform distribution (in size and shape) of ZnO grains is observed from the thin film after thermal annealing for 2 h [2]. It is noted that the deep slits or voids between the grains cause the strong scattering of light in all directions and out of the thin film. However, our experiment has shown that strong lateral confinement of light can be obtained by forming a 2- $\mu\text{m}$ -wide ridge waveguide on the ZnO thin films [2]. This is because the localization length,  $\xi$ , of the highly disordered ZnO thin films is compatible with the width of the ridge waveguide. By using long wavelength approximation [8], it can be shown that  $\xi \approx 2l_s$  where  $l_s$  is the scattering

Manuscript received February 6, 2004; revised April 16, 2004. This work was supported by the Agency for Science, Technology and Research of Singapore under Project 022-101-0033 and by Nippon Sheet Glass Foundation.

The authors are with the School of Electrical and Electronic Engineering, Nanyang Technological University, Singapore 639798 (e-mail: esfyu@ntu.edu.sg).

Digital Object Identifier 10.1109/JQE.2004.833221

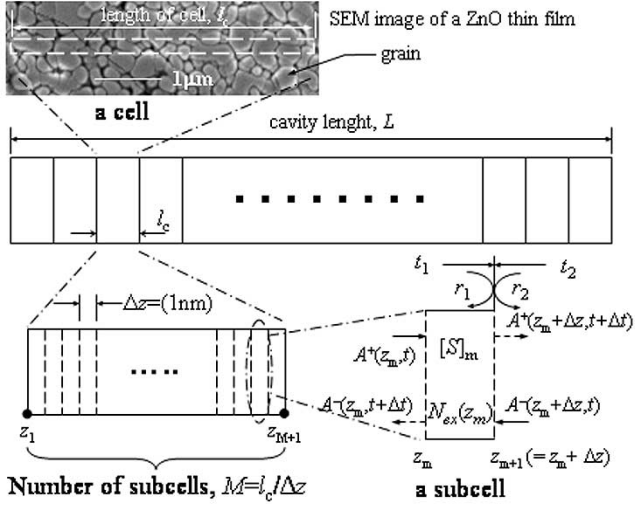


Fig. 1. Schematic of the highly disordered ZnO thin film. The definition of the cells and subcells of the highly disordered media is also indicated.

mean-free path of the thin films. Furthermore, the random laser theory indicates that  $A_{\text{th}}^{2/3} \approx d^{-2/3} l_s 2(\partial g / \partial P)^{-1} P_{\text{th}}^{-1}$  where  $d$  is the thickness of the thin films,  $A_{\text{th}}$  is the threshold excitation area,  $P_{\text{th}}$  is the threshold pump intensity and  $\partial g / \partial P$  is the differential gain. From our experimental investigation, it can be shown that  $d^{-2/3} l_s 2(\partial g / \partial P)^{-1} \approx 4.3 \times 10^{-3} \text{ MWcm}^{2/3}$  [2] and  $\partial g / \partial P \approx 72 \text{ cmMW}^{-1}$  [9]. Hence, the value of  $l_s(\xi)$  is found to be  $\sim 1.1 \mu\text{m}$  ( $\sim 2.2 \mu\text{m}$ ) for  $d = 200 \text{ nm}$ . Our rough estimation of  $\xi$  indicates that strong lateral confinement of light inside the ridge structure is possible as  $\xi > 2 \mu\text{m}$ . Therefore, it is verified that the formation of ridge waveguide in highly disordered ZnO thin films can minimize nonaxial scattering and the analysis of lasing light can be restricted to the axial direction.

### A. Time-Dependent Transfer-Matrix Method

It is assumed that the entire disordered medium, which has a total cavity length of  $L$ , is divided into  $N$  ( $= L/l_c$ ) cells of length  $l_c$  ( $= 1 \mu\text{m}$ ). Each cell is further divided into  $M$  ( $= l_c/\Delta z$ ) subcells of length  $\Delta z$  ( $= 1 \text{ nm}$ ). Here, the subcells are used to construct the random size distribution of grains and voids inside every disordered cell as well as the entire random cavity. The traveling-wave equations describing the propagation of the optical fields inside the thin film can be written as [10]

$$\frac{1}{\nu_g} \frac{\partial A^\pm}{\partial t} \pm \frac{\partial A^\pm}{\partial z} = H(z, t) A^\pm \quad (1)$$

where  $A^+(z, t)$  and  $A^-(z, t)$  are the slowly time-varying envelope of the forward and reverse optical fields, respectively, along the longitudinal direction,  $z$ ,  $t$  is the time,  $\nu_g$  ( $= c/n_g$ ) is the group velocity,  $c$  ( $= 3 \times 10^{10} \text{ cm/s}$ ) is the velocity in free space, and  $n_g$  ( $= 2.3$ ) is the group refractive index of subcells. The function  $H$  can be expressed as  $H = (1/2)((g - \alpha_s) + j n_g k_o)$  where  $j = \sqrt{-1}$ ,  $\alpha_s$  ( $= 80 \text{ cm}^{-1}$ ) is the total scattering and absorption loss in the ZnO grains.  $k_o$  ( $= 2\pi/\lambda$ ) is the wavevector,  $\lambda$  ( $= 390 \text{ nm}$ ) is the free-space wavelength, and  $g$  is the optical gain. If the time and spatial variations of  $A^\pm$  and  $H$  are quantized, (1) can be solved by using the time-

domain traveling-wave method [10]. This can be done by assuming that there are  $N \times M + 1$  pairs of  $A^\pm$  ( $N \times M$  number of  $H$ ) allocated at the boundaries of each subcell (uniformly distributed inside each subcell). Hence, the nonuniform distribution of  $A^\pm$  and  $H$  along  $z$  can be described in a discrete manner. By choosing the relation between variation of time  $\Delta t$  and spatial step  $\Delta z$  as  $\Delta z = \nu_g \times \Delta t$ , which is the restraint of Courant–Friedrich–Levy (CFL) condition of the conventional FDTD method [11], it can be shown that

$$A^\pm(z_m \pm \Delta z, t + \Delta t) \approx [1 + H(z_m, t) \Delta z] A^\pm(z_m, t) \quad (2)$$

where  $z_m$  is the location of subcell boundary.

The reflection and transmission of light at the interface of the subcells can be taken into consideration by using a transfer matrix  $[S]_m$ . The modification of (2) can be written as

$$\begin{aligned} & \begin{bmatrix} A^+(z_m + \Delta z, t + \Delta t) \\ A^-(z_m + \Delta z, t) \end{bmatrix} \\ &= \begin{bmatrix} s_{11}(z_m, t) & s_{12}(z_m, t) \\ s_{21}(z_m, t) & s_{22}(z_m, t) \end{bmatrix} \begin{bmatrix} A^+(z_m, t) \\ A^-(z_m, t + \Delta t) \end{bmatrix} \\ &\equiv [S]_m \begin{bmatrix} A^+(z_m, t) \\ A^-(z_m, t + \Delta t) \end{bmatrix}. \end{aligned} \quad (3)$$

It can be shown that  $[S]_m$  can be written as [8]

$$\begin{aligned} [S]_m &= t_2^{-1} \begin{bmatrix} 1 & r_2 \\ r_2 & 1 \end{bmatrix} \\ &\times \begin{bmatrix} \exp(H(z_m, t) \Delta z) & 0 \\ 0 & \exp(-H(z_m, t) \Delta z) \end{bmatrix} \end{aligned} \quad (4)$$

where  $r_2$  and  $t_2$  are the reflection and transmission coefficients at the interface  $z_{m+1}$ . In order to solve (2) using time-domain traveling-wave method, (3) has to be rewritten in the following format:

$$\begin{aligned} & \begin{bmatrix} A^+(z_m + \Delta z, t + \Delta t) \\ A^-(z_m, t + \Delta t) \end{bmatrix} = s_{22}^{-1} \begin{bmatrix} (s_{11}s_{22} - s_{12}s_{21}) & s_{12} \\ -s_{21} & 1 \end{bmatrix}_m \\ & \times \begin{bmatrix} A^+(z_m, t) \\ A^-(z_m + \Delta z, t) \end{bmatrix}. \end{aligned} \quad (5)$$

For the optical fields emitted from the left (right) facets with reflectivity  $r_L$  ( $r_R$ ), the boundary conditions can be written as  $A^-(z_L, t) = r_L A^+(z_L, t)$  ( $A^+(z_R, t) = r_R A^-(z_R, t)$ ), where  $z_L$  ( $z_R$ ) is the location of the left (right) facets.

Optical gain of ZnO material is due to excitonic and electron–hole–plasma recombination. It is shown that for optical pump intensity less than  $0.7 \text{ MW/cm}^2$ , the optical gain of ZnO materials is mainly contributed by excitonic recombination [12]. In our highly disordered ZnO thin films, since the threshold pump intensity is around  $0.35 \text{ MW/cm}^2$ , the excitonic recombination will be the dominant mechanism. Hence, the recombination process in ZnO thin films can be assumed to depend only on the excitonic recombination. The population dynamics of excitons  $N_{\text{ex}}$  in each subcell can be described by the rate equation of a two-level system as shown below [13]

$$\begin{aligned} \frac{\partial N_{\text{ex}}(z_m, t)}{\partial t} &= \frac{\nu_g P_{\text{pump}}(z_m, t)}{d} \\ & - \frac{N_{\text{ex}}(z_m, t)}{\tau_N} - \nu_g g(N_{\text{ex}}) P(z_m, t) \end{aligned} \quad (6)$$

where  $d(= 200 \text{ nm})$  is total thickness of the thin film and  $\tau_n(= 0.4 \text{ ns})$  is the lifetime of excitons [13].  $P$  is the average photon density inside a subcell and  $P_{\text{pump}}$  is the pump intensity. The time variation of  $N_{\text{ex}}$  can also be approximated by

$$N_{\text{ex}}(z_m, t + \Delta t) = N_{\text{ex}}(z_m, t) + \left. \frac{\partial N_{\text{ex}}(z_m, t)}{\partial t} \right|_t \Delta t. \quad (7)$$

It is noted that there are  $N \times M$  number of  $N_{\text{ex}}$  (i.e., corresponding to  $N \times M$  number of  $H$ ) to be calculated in each time step  $\Delta t$ .

### B. Auxiliary Equations

The net optical gain of our ZnO thin films is shown to be linearly proportional to the pump intensity [9]. Hence, it is reasonable to assume that the optical gain of ZnO thin films has a linear relationship with the exciton population. The optical gain,  $g$ , due to the excitonic recombination can be approximated by  $g(N_{\text{ex}}) = a_N(N_{\text{ex}} - N_0)$  [14] where  $a_N(= 4 \times 10^{-16} \text{ cm}^2)$  is the gain coefficient and  $N_0(= 2.5 \times 10^{18} \text{ cm}^{-3})$  is the excitonic population at transparency.  $a_N$  is roughly estimated from the variable stripe length method and the value of  $N_0$  is assumed to be an order of magnitude less than that of Mott density of ZnO at room temperature [15].

In order to simulate the real laser system, the inhomogeneous distribution of spontaneous emission has to be introduced into the calculation. Spontaneous emission,  $U_{\text{sp}}^{\pm}$ , can be coupled to the optical fields at the interface of the subcells. From (3) and (5), the spontaneous emission  $U_{\text{sp}}^+(z_m, t)$  and  $U_{\text{sp}}^-(z_m + \Delta z, t)$  coupled to  $A^+(z_m, t)$  and  $A^-(z_m + \Delta z, t)$ , respectively, can be written as

$$A^-(z_m, t + \Delta t) = s_{22}^{-1} A^-(z_m + \Delta z, t) - s_{22}^{-1} s_{21} A^+(z_m, t) + U_{\text{sp}}^-(z_m + \Delta z, t), \quad (8a)$$

$$A^+(z_m + \Delta z, t + \Delta t) = s_{11} A^+(z_m, t) + s_{12} A^-(z_m, t + \Delta t) + U_{\text{sp}}^+(z_m, t). \quad (8b)$$

However, we may not need to add  $U_{\text{sp}}^{\pm}$  at every interface. Instead we can add  $U_{\text{sp}}^{\pm}$  between interfaces of distance shorter than  $\xi$  ( $\approx 2.2 \mu\text{m}$ ). This should be accurate enough to simulate random lasing action.  $U_{\text{sp}}^{\pm}$  can be simulated by a Gaussian-distributed random number generator with the required conditions specified in [16]. Furthermore, the optical gain spectrum of ZnO can be modeled by using a digital filter [16]. A possible digital filter with unit gain can be written as  $y_{t+\Delta t} = B y_t + (1 - B)x_t$  where  $y_t$  and  $x_t$  are the output and input of the digital filter at time  $t$ , respectively.  $B$  is the complex number with  $|B| < 1$ . The phase of  $B$  determines the peak gain frequency, and the magnitude of  $B$  determines the bandwidth of the digital filter. As the bandwidth of the amplified spontaneous emission spectra of the ZnO thin films is  $\sim 40 \text{ nm}$ , the corresponding value of  $|B|$  is set to 0.01 [9]. Again, a digital filter is applied between interfaces of distance shorter than  $\xi$ .

The random distribution of ZnO grains can be implemented by assuming that the size of the ZnO grain varies from  $W_{\text{min}} = 40 \text{ nm}$  to  $W_{\text{max}} = 300 \text{ nm}$ . The length of the ZnO grains,  $W$ , can be expressed as  $W = A_1 \gamma^2 + A_2 \gamma + A_3$  where  $\gamma$  is a

random number varying between 0 and 1 [7]. The coefficients  $A_1(= 260)$ ,  $A_2(= -50)$ , and  $A_3(= 40)$  can be deduced by curve fitting with the conditions that when  $\gamma = 0, 0.5$  and  $1.0$ , the corresponding values of  $W$  are  $40 \text{ nm}$ ,  $80 \text{ nm}$  and  $300 \text{ nm}$ , respectively. Therefore, the distribution of ZnO grains can be defined by assigning the appropriate reflectivity at the interfaces of the subcells. The transmission and reflection of light between the ZnO grains and voids are assumed to be due to the difference in refractive indices between the ZnO grains ( $n_{\text{ZnO}} = 2.1$ ) and air ( $n_{\text{air}} = 1$ ). Furthermore, the average length of voids is assumed to be  $3 \text{ nm}$ .

### C. Numerical Technique

$A^{\pm}$  and  $N_{\text{ex}}$  can be solved by integrating (7) and (8) self-consistently over the entire cavity. This can be done by knowing the initial value of  $A^+(z_m, t_0)$  and  $N_{\text{ex}}(z_m, t_0)$  at time  $t_0$ .  $A^+(z_m + \Delta z, t_0 + \Delta t)$  at  $t_0 + \Delta t$  can then be deduced from (8a) by advancing  $A^+(z_m, t_0)$  by a spatial step  $\Delta z$ . Similarly,  $A^-(z_m, t + \Delta t_0)$  can also be evaluated from (8b) by reversing  $A^-(z_m + \Delta z, t_0)$  by a spatial step  $\Delta z$ . Furthermore,  $N_{\text{ex}}(z_m, t_0 + \Delta t)$  at the next time step,  $t_0 + \Delta t$ , can be calculated from (7) at  $t_0$  for each subcell. The iteration process will stop when the required time step is reached. Hence, it is noted that our proposed model is similar to that of the conventional FDTD method.

In order to increase the size of spatial step  $\Delta z$  (as well as sampling time  $\Delta t$ ) for each iteration,  $M$  subcells are multiplied together using  $[S]_m$  to form a cell. It is also assumed that  $N_{\text{ex}}$  is uniformly distributed along the entire  $M$  subcells. This assumption is valid if  $M\Delta z$  is less than the diffusion length  $L_d$  (which is in the order of micrometers) of  $N_{\text{ex}}$  [17]. As a consequence, the total number of rate equations of  $N_{\text{ex}}$  to be solved after the multiplication of  $M$  subcells is reduced by  $M$  times. The advantage of using  $[S]_m$  is that the new spatial step (sampling time) can be increased to  $M\Delta z$  ( $M\Delta t$ ) without affecting the stability and accuracy of the calculation. In addition, the choice of  $M$  will not be limited by the Nyquist criterion as the actual spatial step and sampling time for  $A^{\pm}$  are still  $\Delta z$  and  $\Delta t$ , respectively. The constraints of our proposed model are  $M\Delta z < L_d$  and  $\xi$ . Hence, the selection of  $M = 1000$  (i.e.,  $M\Delta z = 1 \mu\text{m}$ ) is appropriate.

In conventional FDTD method, if  $\Delta z$  is used as the spatial step, the requirement of CFL condition restricts  $\Delta t$  to  $\Delta t = \nu_g / \Delta z$ . The total number of iterations done by the conventional FDTD method will be  $M$  times more than that of our proposed method (with multiplication of  $M$  subcells) for the same stability and accuracy of calculation (i.e., same values of  $\Delta z$  and  $\Delta t$  are used by the two methods). Alternating-direction implicit (ADI) can be applied to eliminate the restraint of the CFL condition in conventional FDTD method so that the sample size (stability) can increase (improve) at the expense of lower calculation accuracy [11]. In addition, the sampling size of ADI FDTD method is limited by the Nyquist criterion: 1) the spatial step should be smaller than the minimum grain size and 2) the time step should be less than half of the resonant period of the random lasers. Therefore, for the same accuracy of calculation, our proposed model can allow larger (lesser) sampling step (iteration) than that of the ADI FDTD method. Therefore, we have shown that our proposed transfer matrix method will

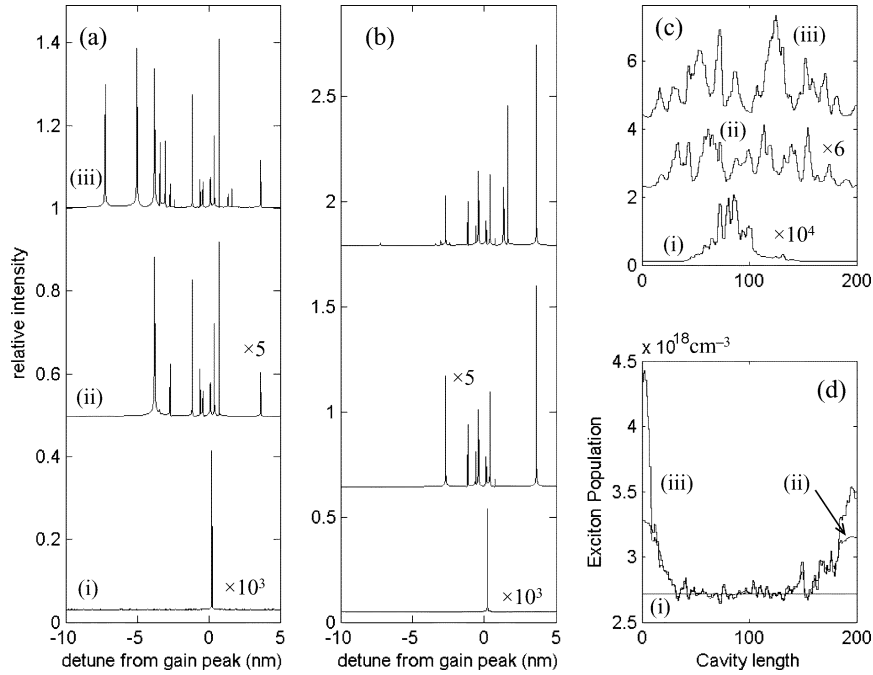


Fig. 2. (a) Spectral intensity emitted from the left facet. (b) Spectral intensity emitted from the right facet. (c) Photon density distribution and (d) exciton population distribution. The pump intensities  $P_{\text{pump}}$  for the cases (i), (ii), and (iii) are  $1.01 \times P_{\text{th}}$ ,  $1.26 \times P_{\text{th}}$ , and  $4.85 \times P_{\text{th}}$ , respectively.

have better computational efficiency than that of the conventional FDTD method. However, further investigation is required to deduce the exact improvement of our proposed transfer matrix method over the conventional FDTD method.

#### D. Numerical Simulation

The proposed model is verified in this section. It is assumed that the highly disordered ZnO thin-film ridge waveguides have cavity length  $L$  of  $200 \mu\text{m}$  and the values of  $r_L$  and  $r_R$  of the laser cavity are set to zero. Fig. 2 shows the lasing spectra (emitted from  $r_L$  and  $r_R$ ) as well as the photon density distribution and exciton population of the highly disordered ZnO thin film under uniform optical pumping for pump intensity varying from  $P_{\text{pump}} = 1.01 \times P_{\text{th}}$  to  $4.85 \times P_{\text{th}}$ , where  $P_{\text{th}}$  is the threshold pump intensity of the random cavity with  $L = 200 \mu\text{m}$ . As expected, the number of lasing modes increases with  $P_{\text{pump}}$  but saturates for  $P_{\text{pump}} > 3.4 \times P_{\text{th}}$ . In addition, the spectra observed from the left facet are different from that of the right facet. Some lasing modes emit from the right facet disappear from the left facet and vice versa. The above calculations have been repeated for 1000 samples with different configuration of randomness. It is noted that the exact positions of the lasing modes are dependent on the configuration of ZnO grains and voids but the dependence of lasing mode behavior on the variation of pump intensity remains unchanged. In addition, the saturated-mode-number varies between 16–20 in the 1000 samples. Hence, we have shown that our simulation results agree with the similar 1-D calculation given in [7] and the proposed transfer matrix model using a two-level rate-equation model can explain the experimental results quantitatively [2].

In our calculations, it is observed that the photon density distribution along the highly disordered thin film is also dependent

on  $P_{\text{pump}}$ . It must be noted that the pattern of photon density distribution is due to the constructive and destructive interference of lasing modes. At low  $P_{\text{pump}}$ , the photon density distribution shows less random. However, when more lasing modes emerge at higher values of  $P_{\text{pump}}$ , the pattern of photon density distribution becomes more random. Hence, it is believed that there is a close relationship between the number of lasing modes and the pattern of photon density distribution. This characteristic of random lasing is similar to that in distributed feedback (DFB) lasers as the band-gap and band-edge modes of DFB lasers show different photon density distributions [18].

An interesting phenomenon in highly disordered media, namely lasing mode redistribution, is also observed from the calculations. The redistribution of lasing modes inside the highly disordered ZnO thin films can be demonstrated by partially pumping the random cavity. Fig. 3 shows the dependence of spectral and spatial distributions of lasing modes on the pump length,  $L_p$ , for  $L_p$  varying from  $20 \mu\text{m}$  to  $160 \mu\text{m}$  with the magnitude of  $P_{\text{pump}}$  remained unchanged at  $3 \times P_{\text{th}}$  ( $P_{\text{th}}$  is the threshold of random cavity with  $L = 200 \mu\text{m}$ ). It is observed that the reduction of  $L_p$  reduces the number of lasing modes emitted from the right facet. As expected, the localized modes at the unpumped region will not be excited (as indicated by arrow  $\leftarrow \circ$ ). However, the reduction of  $L_p$  generates new lasing modes (as indicated by arrow  $\leftarrow \otimes$ ), which dominate new spatial and spectral locations. It is also noted that the spectral distribution of lasing modes is closely related to the photon density distribution. This is again due to the properties of lasing mode localization and repulsion so that the lowest threshold can be maintained for the random cavity. The threshold pump intensity for the random cavity with  $L_p = 20 \mu\text{m}$  is only increased by  $\sim 1.3$  times compared to that of the random cavity with  $L_p = 160 \mu\text{m}$ . This lasing characteristic of random lasers

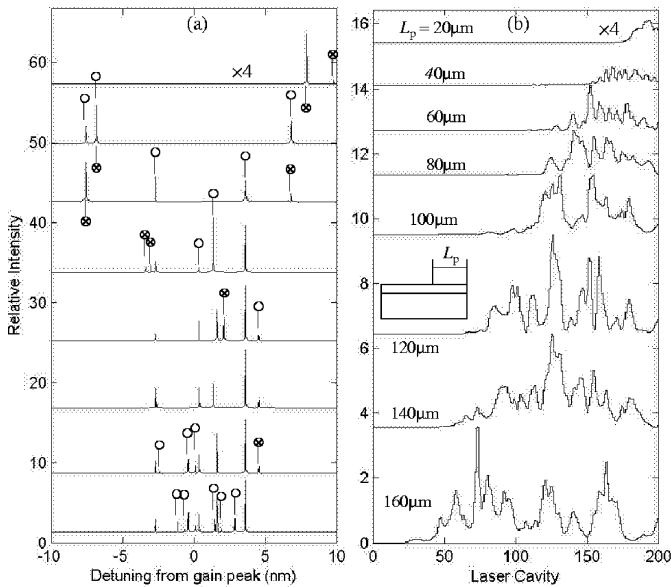


Fig. 3. (a) Spectral intensity emitted from the right facet. (b) Photon density distribution. The pump intensity,  $P_{\text{pump}}$ , is set to  $3 \times P_{\text{th}}$  for the cases where  $L_p$  is varied from 160 to  $20 \mu\text{m}$ .

is quite different from the conventional Fabry–Perot (FP) lasers (i.e., threshold of FP lasers is inversely proportional to the cavity length). On the other hand, if  $P_{\text{pump}}$  increases to  $10 \times P_{\text{th}}$ , it can be shown that the reduction of  $L_p$  reduces the saturated-mode number due to lasing mode repulsion.

### III. COUPLED-CAVITY ZnO THIN-FILM RANDOM LASERS

From the above analysis, it is noted that selective excitation of lasing modes, which can be used to realize high-power single-mode emission, can be obtained by controlling the photon density distribution. Fig. 4 shows the schematic of the coupled-cavity random laser, which consists of a short random cavity (highly disordered ZnO thin film) and a uniform TWA (uniform ZnO thin film). The short random cavity allows single-mode emission and the TWA amplifies the lasing intensity so that high-power single-mode operation can be achieved. It is assumed that the length of the short random cavity  $L_C$  and TWA,  $L_A$ , is  $40 \mu\text{m}$  and  $160 \mu\text{m}$ , respectively.  $L_C = 40 \mu\text{m}$  is selected because this length is easy to handle and has saturated-mode-number less than 5.  $L_A$  is selected to be shorter than the corresponding saturation length. It can be shown that single-mode emission can be achieved in the short random cavity by nonuniform pumping. Previous analysis of random lasers has also shown that the selective excitation of individual localized modes can lead to single-mode operation [7]. However, the required excitation area is less than the localization length and the pump intensity is just slightly above threshold. Here, we use the property of lasing mode redistribution to constrain single-mode emission in random media and single-mode emission will be excited well above threshold.

In the calculation, it is assumed that  $r_L = r_R = 0$  (i.e., the influence of facet reflection will be considered later) and the TWA is pumped uniformly at  $P_{\text{pump}} = 2 \times P_{\text{th}}$ . Fig. 5 shows the lasing characteristics of the proposed random laser under

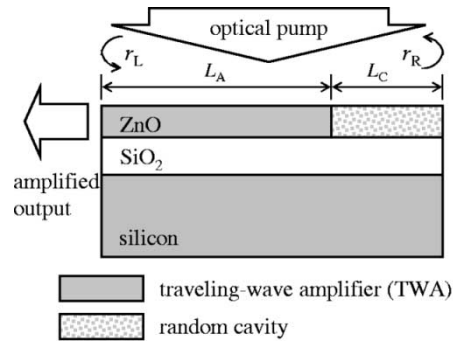


Fig. 4. Novel ZnO thin film laser with traveling wave amplified of length  $L_A$  and highly disordered cavity of length  $L_C$ .

nonuniform pumping and the pumping profile is normalized to 1.0 at the TWA section. In the figure, the lasing modes marked with “A” and “B” represents the lasing modes of the random cavity. It is shown that selective excitation can be realized by nonuniform optical pumping (i.e., lasing mode redistribution). It is required that the pumping profiles to be selected will reduce the number of localization modes (i.e., number of peaks in the photon density distribution) in order to achieve single-mode emission. Furthermore, it is shown that the TWA can increase the single-mode intensity by three times (i.e., see mode “A”) and further enhancement is possible if longer  $L_A$  is used. The above calculation has been repeated for 1000 samples with different random configuration and it is found that single-mode emission can always be obtained with proper selection of pumping profile.

If the coupled-cavity ZnO thin-film laser is fabricated, the corresponding facets will be realized by cleaving. It is expected that the cleaved facets may provide optical feedback to the laser cavity so that the mechanism of selective excitation may be affected. Therefore, the influence of reflectivity and phase of both facets on the spectral and spatial distribution of the lasing modes is studied. In the calculation, it is assumed that both random cavity and TWA are uniformly pumped at  $1.4 \times P_{\text{th}}$  ( $P_{\text{th}}$  is the threshold of random cavity with  $L = 200 \mu\text{m}$ ). The values of  $|r_L|$  and  $|r_R|$  are set to 0.3548 (i.e., perfect smooth facets) in order to clearly demonstrate the influence of optical feedback on the lasing mode redistribution. The calculation has been repeated for 1000 samples with different random configurations. The analysis is summarized below and illustrated with examples.

- It can be shown that destabilization of lasing modes occurs for the magnitude of  $r_L$  and  $r_R$  greater than  $10^{-3}$  and  $10^{-2}$ , respectively. The lasing mode has better resistance to optical feedback from  $r_R$  than that from  $r_L$ . This is because the optical field reflected from  $r_L$  has been amplified by the TWA before re-entering into the random cavity.
- The phase,  $\phi_R$ , represents the uncertainty of distance from the nearest grain to the right facet. Fig. 6 shows the spectral and spatial distribution of the lasing modes for the laser with  $r_L = 0$  and  $r_R = |r_R| \exp(j\phi_R)$  where  $|r_R| = 0.3548$  and  $\phi_R$  varies from 0 to  $\pi$ . The configuration of the random cavity is identical to that used in Fig. 5. It is noted that  $r_R$  causes the generation of modes “C” and “D”

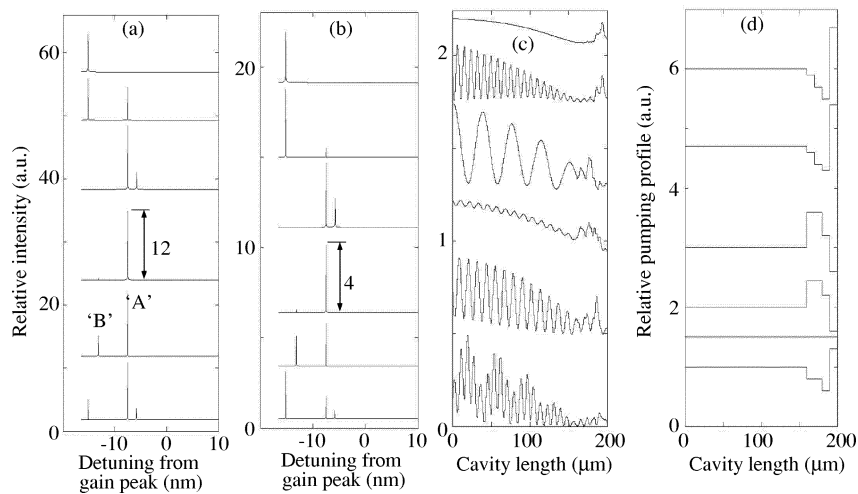


Fig. 5. (a) Spectral intensity emitted from the left facet. (b) Spectral intensity emitted from the right facet. (c) Photon density distribution. (d) Spatial distribution of pump intensity  $P_{\text{pump}}$ , which is normalized by  $2 \times P_{\text{th}}$ .

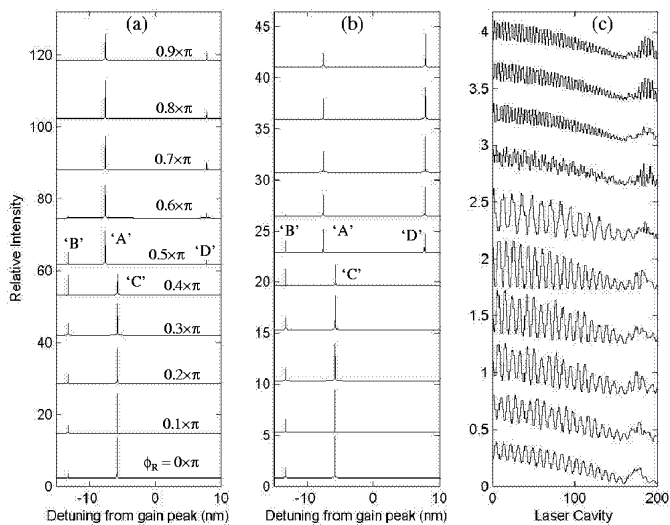


Fig. 6. (a) Spectral intensity emitted from the left facet. (b) Spectral intensity emitted from the right facet. (c) Spatial distribution of photon density. It is assumed that  $r_L = 0$  and  $r_R = 0.5384 \exp(j\phi_R)$  where  $\phi_R$  varies from 0 to  $\pi$ .

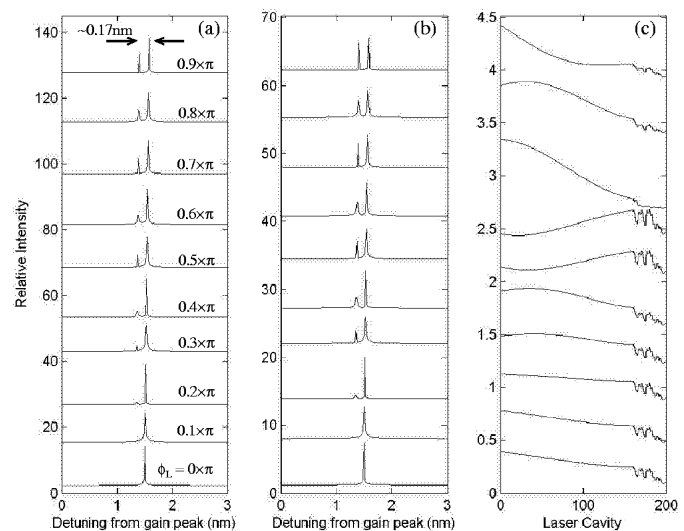


Fig. 7. (a) Spectral intensity emitted from the left facet. (b) Spectral intensity emitted from the right facet. (c) Spatial distribution of photon density. It is assumed that  $r_R = 0$  and  $r_L = 0.5384 \exp(j\phi_L)$  where  $\phi_L$  varies from 0 to  $\pi$ .

as well as elimination of “A” and “B” at some values of  $\phi_R$ . This is due to the lasing mode redistribution so that selective excitation of lasing modes is observed with the variation of photon density distribution. It is also observed that the influence of  $\phi_R$  is equivalent to that of nonuniform pumping. This behavior of lasing mode redistribution is also observed in other random configurations but the exact wavelength of the lasing modes will be different.

- The phase,  $\phi_L$ , represents the uncertainty of distance from the nearest grain to the left facet. Fig. 7 shows the spectral and spatial distribution of the lasing modes for the laser with  $r_R = 0$  and  $r_L = |r_L| \exp(j\phi_L)$  where  $|r_L| = 0.3548$  and  $\phi_L$  varies from 0 to  $\pi$ . The configuration of the random cavity is identical to that used in Fig. 5. It is observed that there are two lasing modes, which are the FP modes sustained by the reflection between  $r_L$  and random cavity, excited with a separation of  $\sim 0.17$  nm. It

is found that the random cavity forms a narrow-band filter with bandwidth of 0.2 nm. This behavior of wavelength filtering is also observed in the case with  $r_R \neq 0$ . In addition, this filtering effect will occur in other random configuration but the exact bandpass wavelength will be different.

- Optical intensity radiating from the left facet can be increased by 4–10 times using the TWA. Further increase in output power is also possible if longer  $L_A$  is used but the maximum length of  $L_A$  is limited by the corresponding saturation power. This value will be investigated by studying the properties of ZnO materials. The influence of  $L_A$  on the spectral and spatial distribution of the lasing modes will be similar to that of  $\phi_L$  and so is not repeated.
- It is observed that the spectral and spatial distributions of lasing modes inside the random cavity are closely related. In Fig. 6, lasing modes “B” and “C” are only excited for

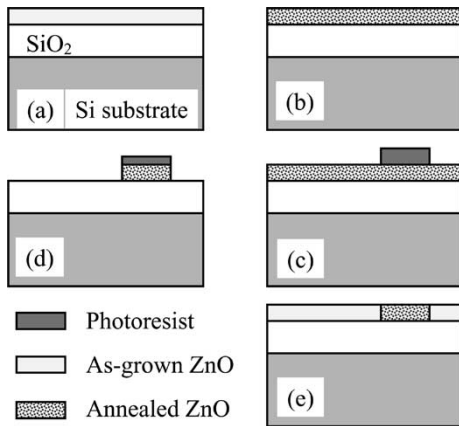


Fig. 8. Fabrication procedures of the proposed coupled-cavity random laser. (a) Deposition of ZnO thin film on SiO<sub>2</sub> buffer layer by FCVA technique. (b) The entire sample undergone thermal annealing. (c) Deposition of line on the annealed ZnO thin film for the preparation of wet etching. (d) Formation of short random cavity after wet etching. (e) Re-deposition of ZnO thin film on the sample and removal of photoresist.

$\phi_R$  varying between 0 and 0.4, and the corresponding pattern of the photon density distributions show similar in shape. However, for  $\phi_R = 0.5$ , both spectral and spatial distribution of lasing modes change significantly. This observation is also true for  $\phi_R$  varying between 0.6–0.9. On the other hand, the lasing modes in Fig. 7 are the FP modes and so the similarity in lasing mode pattern is not observed.

From the above analysis, it is noted that the influence of  $r_R$  can be resolved by nonuniform pumping as the lasing modes are only affected by  $r_R$ . On the other hand, the presence of  $r_L$  generates FP modes, which can also be suppressed by nonuniform pumping. Our previous study, however, has shown that high optical feedback may not be easily obtained in ZnO thin films by cleaving as in the case of (100) GaAs or InP semiconductor materials. It is estimated that the field reflectivity of the cleaved facets has a value less than  $10^{-3}$  [9]. Therefore, if  $L_A$  is not too long, single-mode emission should be able to realize in coupled-cavity laser with nonuniform pumping to control the selective excitation of lasing modes.

#### IV. EXPERIMENTAL RESULTS

The coupled-cavity ZnO thin-film random laser can be fabricated by our post-growth annealing technique [2]. The fabrication procedures (see also Fig. 8) are described as follows.

- A 180-nm-thick ZnO thin film was deposited by FCVA technique on a Si substrate with SiO<sub>2</sub> (of thickness  $\sim 400$  nm) as the buffer layer. During the deposition, substrate temperature and oxygen partial pressure were set to 230 °C and  $2 \times 10^{-4}$  torr, respectively.
- The ZnO thin film underwent post-growth annealing at 900 °C for 2 h in open air.
- A photoresist stripe, which has a width of 40  $\mu\text{m}$ , was formed on the surface of the annealed ZnO thin film by photolithography technique.

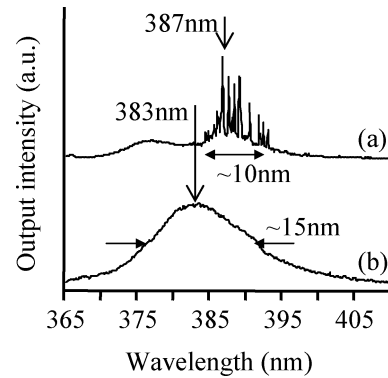


Fig. 9. Emission spectra of the (a) annealed and (b) as-grown ZnO thin films at pump intensity of  $\sim 1.5$  MW/cm<sup>2</sup>.

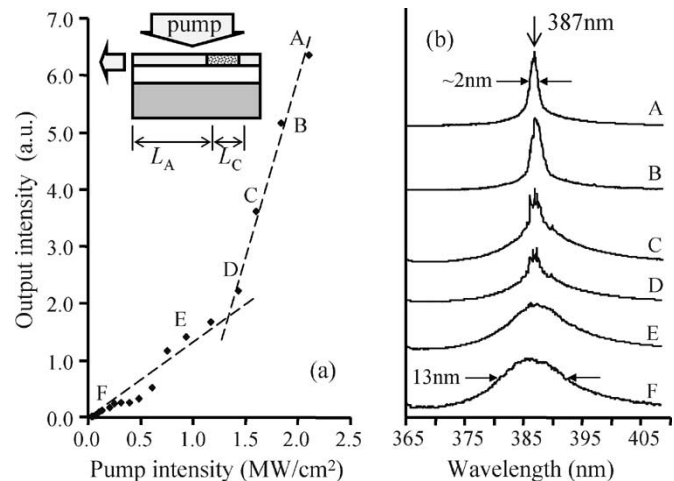


Fig. 10. (a) Light-light curve for the ZnO thin film coupled-cavity random laser. (b) Corresponding emission spectra at vary pump intensities.

- The unmasked region of the annealed ZnO thin film was completely removed by wet etching using diluted HCl solution.
- A 220-nm-thick ZnO thin film was re-deposited on the sample by FCVA technique at the same deposition conditions as described above. After the deposition, the remaining photoresist was removed.

As a result, a coupled-cavity ZnO thin film random laser is fabricated on Si substrate with  $L_A \approx \sim 0.2$  cm and  $L_C \approx \sim 40$   $\mu\text{m}$ .

Room-temperature optical-characteristics of the ZnO thin film random laser were studied under optical excitation by a frequency-tripled Nd:YAG laser (at 355 nm) at pulsed operation (6 ns, 10 Hz). Optical pump was achieved by using a cylindrical lens to focus a pump stripe of length 5 mm and width 8  $\mu\text{m}$  on to the sample. Fig. 9 shows the emission spectra from the as-grown and annealed ZnO thin films at excitation intensity of  $\sim 1.5$  MW/cm<sup>2</sup>. It is observed that the as-grown sample has a single-broad spontaneous emission spectrum with peak wavelength and full-width half-maximum of  $\sim 383$  nm and  $\sim 13$  nm, respectively. On the other hand, sharp peaks (i.e., lasing modes at  $\sim 387$  nm) with linewidth less than 0.4 nm emerged from the emission spectrum of the annealed ZnO sample. These indicate that our as-grown and annealed ZnO thin film exhibit amplified spontaneous emission and coherent random lasing, respectively, as expected [2], [9].

Fig. 10 shows the light–light curve and emission spectra of the coupled-cavity random laser. A kink at pump intensity of  $\sim 1.3 \text{ MW/cm}^2$  is observed from the light–light curve. In addition, the spectral linewidth reduces from  $\sim 13 \text{ nm}$  to  $\sim 2 \text{ nm}$  as the input pump intensity increases about the kink. The presence of the kink accompanied by a narrowing of the spectral linewidth suggests the sample exhibit random lasing. It is also observed that the narrowing of the emission spectra (“C” and “D”) are caused by the merging of sharp peaks. It is noted that the peak wavelength of the emission spectra ( $\sim 378 \text{ nm}$ ) is consistent with the peak emission wavelength of the random lasing spectrum as shown in Fig. 9. Hence, it is shown that the sharp peaks emitted from the short random cavity are under amplification as well as linewidth broadening inside the TWA. In addition, it is shown that the design of coupled-cavity random laser can minimize the number of lasing modes. This is because the short random cavity only supports few sharp peaks as expected from the calculation given in Section II-D. Comparison between the spectra width given in Fig. 9(a) ( $\sim 10 \text{ nm}$ ) and that given in Fig. 10(b) curve “A” ( $\sim 2 \text{ nm}$ ) supports our claim. Furthermore, it is found that the facets of the coupled-cavity laser are too rough (too low reflectivity) to sustain FP modes [9]. Thus, we have shown that 1) the sharp peaks from the short random cavity can be amplified by the TWA of the coupled-cavity laser and 2) the number of sharp peaks are limited by the design of short random cavity. Therefore, our experimental results verified our idea of using coupled-cavity random laser to realize high-power single-mode operation. The possibility of using nonuniform optical pumping to obtain single-mode operation will be studied in our future publication.

## V. CONCLUSION

In conclusion, an effective time-domain traveling-wave model was developed to simulate the random lasing action of highly disordered ZnO thin films. The simulation program is written in Fortran 95 run on an IBM compatible Pentium 4 PC with 3-GHz clock rate. It takes about 2 min to simulate 1 ns transient response for a random cavity with  $L$  and  $\Delta z(\Delta t)$  of  $200 \mu\text{m}$  and  $1 \text{ nm}$  ( $0.077 \text{ fs}$ ), respectively. From our numerical calculation, we have found that the properties of lasing mode redistribution can be used to achieve single-mode operation in highly disordered media. Lasing modes inside the random cavity can be generated or eliminated by controlling the corresponding photon density distribution. A coupled-cavity random laser, which consists of a short random cavity and a TWA, is proposed to achieve high-power single-mode operation. Theoretical studies have shown that single-mode operation can be easily achieved inside the random cavity with nonuniform optical pumping and the influence of  $r_R$  can be compensated by alternating the profile of optical pumping. This is because nonuniform optical pumping controls the photon density distribution so that selective excitation of individual localized modes can be achieved. On the other hand, FP modes can be excited by the presence of  $r_L$ , due to the formation of FP cavity inside the TWA through the optical feedback from

$r_L$  and the highly disordered media, so that it is necessary to maintain the magnitude of  $r_L$  less than  $10^{-3}$ . Our preliminary experimental results have proved that: 1) the lasing modes from the short random cavity can be amplified by the TWA and 2) the number of lasing modes can be limited by the design of short random cavity. Hence, the possibility to realize high-power single-mode operation in highly disordered ZnO thin films using the coupled-cavity design is verified.

## REFERENCES

- [1] H. Cao, Y. G. Zhao, S. T. Ho, E. W. Seeling, Q. H. Wang, and R. P. H. Chang, “Random laser action in semiconductor powder,” *Phys. Rev. Lett.*, vol. 82, no. 11, pp. 2278–2281, 1999.
- [2] S. F. Yu, C. Yuen, S. P. Lau, and H. W. Lee, “Zinc oxide thin-film random lasers on silicon substrate,” *Appl. Phys. Lett.*, vol. 84, no. 17, pp. 3244–3246, 2004.
- [3] H. Cao, J. Y. Xu, D. Z. Zhang, S. H. Chang, S. T. Ho, E. W. Seeling, X. Liu, and R. P. H. Chang, “Spatial confinement of laser light in active random media,” *Phys. Rev. Lett.*, vol. 84, no. 24, pp. 5584–5587, 2000.
- [4] J. M. Bian, X. M. Li, X. D. Gao, W. D. Yu, and L. D. Chen, “Deposition and electrical properties of N-In codoped p-type ZnO films by ultrasonic spray pyrolysis,” *Appl. Phys. Lett.*, vol. 84, no. 4, pp. 541–543, 2004.
- [5] R. M. Balachandran, A. E. Perkins, and N. M. Lawandy, “Injection locking of photonic paint,” *Opt. Lett.*, vol. 21, no. 9, pp. 650–652, 1996.
- [6] P. Sebbah and C. Vanneste, “Random laser in the localized regime,” *Phys. Rev. B*, vol. 66, pp. 144 202-1–144 202-10, 2002.
- [7] X. Jiang and C. M. Soukoulis, “Time dependent theory for random lasers,” *Phys. Rev. Lett.*, vol. 85, no. 1, pp. 70–74, 2000.
- [8] Z. Q. Zhang, “Light amplification and localization in randomly layered media with gain,” *Phys. Rev. B*, vol. 52, no. 11, pp. 7960–7964, 1995.
- [9] S. F. Yu, C. Yuen, S. P. Lau, Y. G. Wang, H. W. Lee, and B. K. Tay, “Ultraviolet amplified spontaneous emission from zinc oxide ridge waveguides on silicon substrate,” *Appl. Phys. Lett.*, vol. 83, no. 21, pp. 4288–4290, 2003.
- [10] S. F. Yu, “An improved time-domain traveling-wave model for vertical-cavity surface-emitting lasers,” *IEEE J. Quantum Electron.*, vol. 34, pp. 1938–1948, Oct. 1998.
- [11] T. Namiki, “A new FDTD algorithm based on alternating direction implicit method,” *IEEE Trans. Microwave Theory Tech.*, vol. 47, pp. 2003–2007, Oct. 1999.
- [12] D. M. Bagnall, Y. F. Chen, Z. Zhu, T. Yao, M. Y. Shen, and T. Goto, “High temperature excitonic stimulated emission from ZnO epitaxial layers,” *Appl. Phys. Lett.*, vol. 73, no. 8, pp. 1038–1040, 1998.
- [13] A. Yamamoto, K. Miyajima, T. Goto, H. J. Ko, and T. Yao, “Biexciton luminescence in high-quality ZnO epitaxial thin films,” *J. Appl. Phys.*, vol. 90, no. 10, pp. 4973–4976, 2001.
- [14] J. Ding, H. Jeon, T. Ishihara, M. Hagerott, and A. V. Nurmikko, “Excitonic gain and laser emission in ZnSe-based quantum wells,” *Phys. Rev. Lett.*, vol. 69, no. 11, pp. 1707–1710, 1992.
- [15] Y. F. Chen, N. T. Tuan, Y. Segawa, H. J. Ko, S. K. Hong, and T. Yao, “Stimulated emission and optical gain in ZnO epilayers grown by plasma-assisted molecular-beam epitaxy with buffers,” *Appl. Phys. Lett.*, vol. 78, no. 11, pp. 1469–1471, 2001.
- [16] L. M. Zhang, S. F. Yu, M. C. Nowell, D. D. Marcenac, J. E. Carroll, and R. G. S. Plumb, “Dynamic analysis of radiation and side mode suppression in second order DFB lasers using time-domain large-signal traveling wave model,” *IEEE J. Quantum Electron.*, vol. 30, pp. 1389–1395, June 1994.
- [17] F. M. Hossain, J. Nishii, S. Takagi, A. Ohtomo, T. Fukumura, H. Fujioka, H. Ohno, H. Koinuma, and M. Kawasaki, “Modeling and simulation of polycrystalline ZnO thin-film transistors,” *J. Appl. Phys.*, vol. 94, no. 12, pp. 7768–7777, 2003.
- [18] S. F. Yu, L. M. Zhang, R. G. S. Plumb, and J. E. Carroll, “Effect of external reflectors on radiation profile of grating coupled surface emitting lasers,” *Proc. IEE-Optoelectron.*, pt. J, vol. 140, no. 1, pp. 30–38, 1993.



**S. F. Yu** (M'03–SM'03) received the Bachelor of Engineering degree from University College, London University, London, U.K., in 1990, and the Doctor of Philosophy degree from Robinson College, Cambridge University, Cambridge, U.K., in 1993.

Currently, he is an Associate Professor in the School of Electrical and Electronic Engineering, Nanyang Technological University, Singapore. His main research interest includes the fundamental study, design, and optimization of semiconductor lasers, including distributed feedback lasers and vertical-cavity surface-emitting lasers. Recently, he was involved in the design and fabrication of zinc oxide thin-film lasers emitted at ultraviolet wavelength. He has published over 100 international technical papers, including invited conference and journal papers, two book chapters, as well as one book, *Analysis and Design of Vertical Cavity Surface Emitting Lasers* (New York: Wiley, 2003).

Dr. Yu was a Guest Editor of the IEEE JOURNAL OF SELECTED TOPICS IN QUANTUM ELECTRONICS in the area of "Optoelectronics Device Simulation" for the May/June 2003 issue. He is a Committee Member of the IEEE/LEOS Conference "Numerical Simulation of Optoelectronic Devices" to be held at the University of California at Santa Barbara in August 2004. He is also the Program Co-Chair of the Symposium N: ZnO and Related Materials, 3rd International Conference on Materials for Advanced Technologies, to be held in Singapore in 2005.

**Eunice S. P. Leong** received the B.Eng. degree in 2003 from Nanyang Technological University, Singapore, where she is currently working toward the Ph.D. degree.

Her research interests are the design and fabrication of ultraviolet light-emitting devices and lasers using wide bandgap materials using sol gel and filtered cathodic vacuum arc techniques.